Host–guest chemistry of rotaxanes and catenanes: application of a polarizable all-atom force field to cyclobis(paraquat-*p*-phenylene) complexes with disubstituted benzenes and biphenyls†

George A. Kaminski and William L. Jorgensen*

Department of Chemistry, Yale University, New Haven, Connecticut 06520-8107, USA

Modeling of host–guest complexes of cyclobis(paraquat-*p*-phenylene) with benzidine, biphenol, 1,4-diaminobenzene, and benzohydroquinone in the gas-phase and in liquid CH_3CN solution with molecular mechanics and Monte Carlo statistical mechanics has been performed. The complexes are important structural elements for a wide variety of self-assembling rotaxanes and catenanes with prospective use in nanoscale devices. However, their highly charged nature presents potential challenges for accurate modeling. In particular, the need for explicit polarization has been considered through computation of association energies using an all-atom force field with and without non-additive electrostatic polarization terms. The effect of including PF_6^- counterions has also been addressed. Polarization generally strengthens the gas-phase interactions, but has modest effects on the structures of the complexes and on the relative free energies of binding in solution, which are in reasonable agreement with experimental data.

Introduction

Molecular dynamics and Monte Carlo techniques have become powerful tools in modern chemistry. They allow the study of structures of molecular systems at the atomic level, computation of energetic properties of condensed-phase systems, and analysis of the nature of chemical processes ranging from solvation of simple molecules to protein stability and ligand binding in solution.[1] The quality of the computational representation of real molecular systems is greatly affected by using an accurate way to compute the potential energy of the molecular interactions. While in many cases, the simple and easily transferable Coulomb and Lennard-Jones formalism is sufficient, provided that careful parameterization has been carried out prior to the target calculations, this standard way to represent intermolecular interactions shows significant drawbacks in some instances. For example, the interaction of cations with molecules containing aromatic rings is poorly reproduced with classical force fields. Specifically, the magnitudes of gas-phase association energies for complexes of benzene with Li^+, Na^+, K^+, and NH_4^+ are underestimated by about a factor of two.[2] This problem can be solved by introducing a non-additive electrostatic energy term depending on the permanent electrostatic charges and induced dipoles at polarizable atomic sites. Such models have been used, for example, to successfully compute properties of pure water,[3] interaction energies for Na^+ with peptides,[4] and free energies of hydration for atomic ions.[5] In these calculations polarization contributed significantly to their success.

Another class of systems in which a non-additive electrostatic term is potentially important is represented by some rotaxanes and catenanes. Due to the recent advances in synthetic supramolecular chemistry, such complexes have become readily available *via* self-assembly procedures.[6] This allows preparation of nanoscale complexes of mechanically interlocked, yet not covalently bound molecules. Such systems have interesting mechanoelectric properties allowing creation of electro- and photochemically controllable molecular shuttles to be used as a basis for nanoscale molecular switches and

information storing devices. Rotaxanes and catenanes are often constructed as complexes of an electron-deficient molecular "bead" sliding along a "thread" or ring with one or more electron-rich stations.[6,7] Having two similar donors in the same thread leads to a molecular shuttle as the "bead" slides back and forth between the stations at the thermally controlled rate and spends an equal amount of time at both of them. This new type of rearrangement is termed "translational isomerisation". Introducing an electron donor with lower oxidation potential and thus with higher donating ability in the same thread makes the electron-deficient unit spend more time near this station, while oxidizing this donor may switch the equilibrium towards the other end.

One of the most commonly used electron-deficient "beads" is cyclobis(paraquat-*p*-phenylene) (**1**).[6–8] It is a relatively rigid
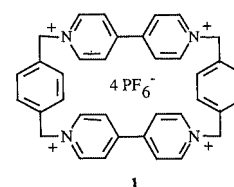
molecule and its central cavity is able to accommodate substituted benzenes and biphenyl derivatives. When electron rich molecules such as benzidine, biphenol, 1,4-diaminobenzene, and hydroquinone (**2**, **3**, **4**, and **5**, respectively) are linked by
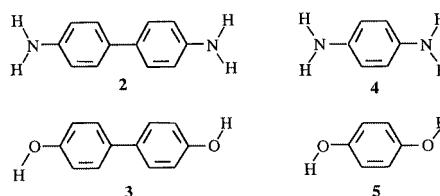
polymethylene chains, they provide the stations. This allows successful self-assembly of a variety of rotaxanes and catenanes.[9] In addition, **2**–**5** are able to bind to the "bead" **1** as simple single molecules, forming 1:1 complexes in CH_3CN solutions.[10,11]

While such complexes have been studied extensively in crystalline form with X-ray diffraction,[12] their structures in solution are not well established. Available experimental data are usually restricted to visible and IR spectra indicating formation of complexes and NMR results including applications of NOE techniques, which allow rough estimation of average interatomic distances.[10,11] Consequently, molecular modeling of rotaxanes, catenanes, and the host–guest complexes that they are built upon is desirable to provide a more detailed understanding of the energetic and structural properties of the complexes. Furthermore, results of computer simulations can help classify the intermolecular interactions primarily responsible for the molecular recognition in rotaxanes and catenanes and their constituent complexes. There is controversy in this regard and different authors have emphasized electrostatics and either charge transfer or polarization as the key elements of the binding.[10–14]

The size of the complexes does not allow modeling with advanced *ab initio* quantum mechanical methods, and even if it did, thermally averaged information in solution is most desirable.[13] Thus, Monte Carlo (MC) statistical mechanics with an empirical force field can be considered as an alternative means of investigation here. However, the host **1** has a +4e electrostatic charge. Also, both the host and the guests are built mostly of aromatic fragments. Therefore, attention to the non-additive polarization interactions is necessary.[13] Solving the problem of choosing the adequate potential energy formalism for this class of molecular systems should allow future computational studies as a complement to the synthesis of new supramolecular systems.

The work presented here addresses the methodology for molecular modeling of rotaxanes and catenanes. Energy minimizations of the **1–2**, **1–3**, **1–4**, and **1–5** complexes in the gas phase as well as determination of their relative free energies of association in acetonitrile have been pursued with molecular mechanics and Monte Carlo calculations using force fields including and excluding non-additive polarization. The effect of including four PF_6^- counterions is also addressed. The importance of taking into account thermal motion as in Monte Carlo simulations or molecular dynamics is also demonstrated.

Computational details

Force field

The energy of non-additive electrostatic polarization, E_{pol}, was included in the total energy expression (1). Here E_{intra} represents

$$E_{total} = E_{intra} + E_{intra}^{NB} + E_{inter}^{NB} + E_{pol} \qquad (1)$$

intramolecular bond-stretching, angle-bending, and torsional energy [eqn. (2)], E_{intra}^{NB} and E_{inter}^{NB} are the intra- and inter-

$$E_{intra} = E_{bond} + E_{angle} + E_{torsion} \qquad (2)$$

molecular Lennard-Jones and charge–charge electrostatic energies. Calculations were also carried out with the polarization energy left out.

All internal degrees of freedom except those within the aromatic rings were sampled in the host. The only internal sampling for the guests was done for rotation of the NH_2 and OH groups and of the *p*-phenylene rings with respect to each other. The almost rectangular shape of host **1** suggests a significant strain, so that sampling the angle bending and bond stretching seemed advisable in this case.

$$E_{bond} = \sum_{bonds} K_r (r - r_{eq})^2 \qquad (3)$$

$$E_{angle} = \sum_{angles} K_\theta (\theta - \theta_{eq})^2 \qquad (4)$$

The energies of the bond stretching and angle bending are

Table 1 Bond stretching and angle bending parameters

Bond or angle	r_{eq}/Å or θ_{eq}/degrees	K_r/kcal (mol Å²)$^{-1}$ or K_θ/kcal (mol rad²)$^{-1}$
HC–CT	1.090	331.0
N$^+$–CT	1.475	337.0
CA(benzene)–CT	1.510	317.0
C!–C!^{a}	1.495	317.0
CA–C!–C!^{a}	120.8	70.0
CA–N$^+$–CT	119.8	70.0
N$^+$–CT–HC	109.5	35.0
HC–CT–HC	109.5	35.0
HC–CT–CA	109.5	35.0
CA–CA–CA	120.0	70.0
CA–CT–N$^+$	114.0	63.0

^{a} The bonds and bond angles between the two pyridinium rings of the host.

Table 2 Fourier coefficients (kcal mol^{-1}) for the torsional energy

Dihedral	V_1	V_2	V_3	V_4
CT–CA–CA–CA (improper)	0.0	10.0	0.0	0.0
HC–CT–CA–CA	0.0	0.0	0.0	0.0
HC–CT–N$^+$–CA	0.0	0.0	0.0	0.0
CA–C!–C!–CA^a	0.0	0.029	0.0	−0.370
C!–C!–CA–CA (improper)^a	0.0	100.0	0.0	0.0
N$^+$–CT–CA–CA	0.0	0.0	0.0	0.0
CA–CT–N$^+$–CA	0.0	0.0	0.0	0.0
CT–N$^+$–CA–CA (improper)	0.0	100.0	0.0	0.0
CA–CA–OH–HO	0.0	3.50	0.0	0.200
CA–CA–N(NH$_2$)–X^b	0.0	3.540	0.0	0.0

^{a} The dihedral angles between the two pyridinium rings of the host or benzene rings of biphenyls. ^{b} X is a dummy atom positioned exactly between the two H atoms of the guest's NH$_2$.

treated harmonically [eqns. (3), (4)]. Values of the constants K_r and K_θ were taken from the AMBER all-atom force field[15] with the exception of bond angles centered at the pyridinium nitrogen and the opposite carbon atoms. These angles had their equilibrium value adjusted to have zero angle bending energy when the whole ring was planar (Table 1).

The torsional energy, $E_{torsion}$, was computed according to eqn. (5), for the dihedral angles, φ_i, where V_1, V_2, V_3, and V_4 are Fourier coefficients. Note that the Fourier series in eqn. (5)

$$E_{torsion} = \sum_i \frac{V_1^i}{2}[1 + \cos(\varphi_i)] + \frac{V_2^i}{2}[1 - \cos(2\varphi_i)] + \frac{V_3^i}{2}[1 + \cos(3\varphi_i)] + \frac{V_4^i}{2}[1 - \cos(4\varphi_i)] \qquad (5)$$

contains a V_4 term which is usually not taken into account.[16–18] It is necessary for accurately reproducing biphenyl-type torsions which are present in both the host **1** and benzidine and biphenol guests, **2** and **3**.[19] Values of all the bond stretching, angle bending and torsional parameters are given in Tables 1 and 2.

The standard Coulomb plus Lennard-Jones formalism was used to compute the non-bonded pairwise-additive part of the intramolecular and intermolecular interactions. For the interactions between molecules (or molecular fragments) a and b eqn. (6) applies. The summation is over all interacting pairs of

$$E_{ab} = \sum_i^{on\ a} \sum_j^{on\ b} [q_i q_j e^2/r_{ij} + 4\varepsilon_{ij}(\sigma_{ij}^{12}/r_{ij}^{12} - \sigma_{ij}^6/r_{ij}^6)]f_{ij} \qquad (6)$$

atomic sites i and j in a and b, and the standard combining rules

Table 3 Lennard-Jones parameters, atomic charges, and polarizabilities

Atom	q/electrons	ε/kcal mol^{-1}	σ/Å	α/Å$^{3\,a}$
CA, benzene	−0.115	0.070	3.55	1.739
CA(CA–CH$_2$)	0.1534	0.070	3.55	1.352
HA(benzene)	0.115	0.030	2.42	—
CT(-CH$_2$-)	−0.1942	0.066	3.50	1.835
HC(-CH$_2$-)	0.1534	0.030	2.50	—
N$^+$	−0.0232	0.170	3.25	1.030
C$^{1\,b}$	0.1652	0.070	3.55	1.739
C$^{2\,b}$	−0.2798	0.070	3.55	1.739
C$^{3\,b}$	0.2604	0.070	3.55	1.352
H^1 on C^1	0.1753	0.030	2.42	—
H^2 on C^2	0.1877	0.030	2.42	—
CA, guest^c	0.0	0.070	3.55	1.352
CA, (CA–NH$_2$)	0.100	0.070	3.55	1.352
CA, (CA–OH)	0.150	0.070	3.55	1.352
N(-NH$_2$)	−0.900	0.170	3.25	1.864
H(-NH$_2$)	0.400	0.0	0.0	—
O(-OH)	−0.585	0.170	3.07	1.024
H(OH)	0.435	0.0	0.0	—
P, PF$_6^-$	1.340	0.200	3.7400	—
F, PF$_6^-$	−0.390	0.061	3.1181	—

^{a} Ref. 21. ^{b} In the pyridinium rings. ^{c} C^1 in biphenyls.

(7) and (8) were employed. The scaling factor $f_{ij} = 1.0$ except for

$$\varepsilon_{ij} = (\varepsilon_{ii}\varepsilon_{jj})^{1/2} \qquad (7)$$

$$\sigma_{ij} = (\sigma_{ii}\sigma_{jj})^{1/2} \qquad (8)$$

the intramolecular 1,4-interactions which were scaled with $f_{ij} = 0.5$. 1,2 and 1,3 non-bonded interactions are disregarded.[16]

All Lennard-Jones σ and ε parameters and electrostatic charges for the guests and for the host p-phenylene rings were taken from the OPLS-AA force field.[16] Charges on the pyridinium groups of the host were obtained by fitting to the electrostatic potential surface (EPS) with the CHELPG procedure using 6-31+G* *ab initio* calculations; they are shown below (in electrons). Such CHELPG charges have been shown to be
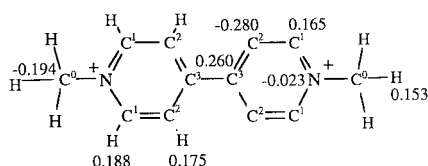
superior to Mulliken charges in reproducing experimental data for host–guest complexes in solution and for single solvated molecules.[17,20] The same procedure was followed in obtaining charges for the PF$_6^-$ counterions. All the atomic parameters are listed in Table 3.

Non-additive electrostatic polarization

The electrostatic polarization energy of the system, whenever included, was calculated from eqn. (9),[4] where $\vec{\mu}_j$ represents the

$$E_{\text{pol}} = -\tfrac{1}{2}\sum_j \vec{\mu}_j \, E_i^0 \qquad (9)$$

induced dipole moment at the ith polarizable atomic site and E_i^0 is the electrostatic field created by the permanent electrostatic charges at its position.

The induced dipoles are determined from eqn. (10), where E_i

$$\vec{\mu}_i = a_i E_i \qquad (10)$$

is the total electrostatic field originating from both the permanent charges and other induced dipoles at the position of the

induced dipole [eqns. (11)–(13)]. This leads to matrix equation

$$E_i = E_i^0 + \sum_j T_{ij}\vec{\mu}_j \qquad (11)$$

$$E_i^0 = \sum_j q_i R_{ji}/R_{ji}^3 \qquad (12)$$

$$T_{ij} = R_{ij}^{-3}\,[3R_{ij} \times (R_{ij}/R_{ij}^2) - 1] \qquad (13)$$

(14) for finding the $\vec{\mu}_j$ to be used in eqn. (9). Eqn. (14) can be

$$A\vec{\mu} = E^0 \qquad (14)$$

$$A_{ij} = \delta_{ij}a_i^{-1} - (1 - \delta_{ij})\,T_{ij} \qquad (15)$$

solved exactly, but solving it iteratively is known to significantly reduce computational time,[3–5] so the latter method was employed in this work. The resulting $\vec{\mu}_j$ are used in eqn. (9) to compute the polarization energy which is then included in the expression for the total energy. Only heavy atoms in the host and the guests were considered to be polarizable. Also, only electrostatic charges of the host, guest, and counterions were taken into account when computing E_i^0. This was done for computational efficiency in the liquid-phase MC calculations as solvent moves then do not affect the polarization energy and thus do not require the time-consuming procedure for its calculation. This makes it necessary to recompute E_i^0, solve eqn. (14), and use eqn. (9) to find the new value of the polarization energy only if a solute (host, guest, or counterion) has moved. Such a restriction can be justified by the fact that the host–guest interactions are the strongest ones in the system and the normally sufficient electrostatic and Lennard-Jones force field should be adequate to describe the solute–solvent and solvent–solvent interaction energies.

Furthermore, the host and the guests were divided into molecular fragments and no two atoms inside the same fragment were taken to interact *via* non-bonded or polarization energy terms.
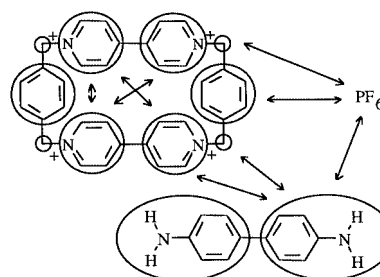
To prevent unphysical growth of E_{pol} when R_{ij} becomes small and the point-dipole approximation used in eqns. (9)–(15) is no longer valid, cutoff rule (16) is imposed. For each atomic pair i

$$R_{ij} = R_{ij} \text{ if } R_{ij} > R_{\text{cutoff}}{}^{ij}, \quad R_{ij} = R_{\text{cutoff}}{}^{ij}; \text{ otherwise} \quad (16)$$

and j, $R_{\text{cutoff}}{}^{ij}$ is assumed to be equal to a parameter γ multiplied by the sum of the van der Waals radii of atoms i and j (Lennard-Jones σ divided by $2^{5/6}$). To find the best value for γ and to test the present polarization model, gas-phase energy minimizations were carried out for complexes of benzene with Na$^+$, aniline with Na$^+$, phenol with Na$^+$, and pyridinium ion with water using *ab initio* calculations at the MP2/6-31G*//6-31G* level and the force field described above. The GAUSSIAN92 program was used for the quantum mechanical calculations.[22] In all the cases, the Na$^+$ and the water oxygen atom positions were restricted to be on a line normal to the plane of the aromatic ring and passing through its center (Fig. 1). It was
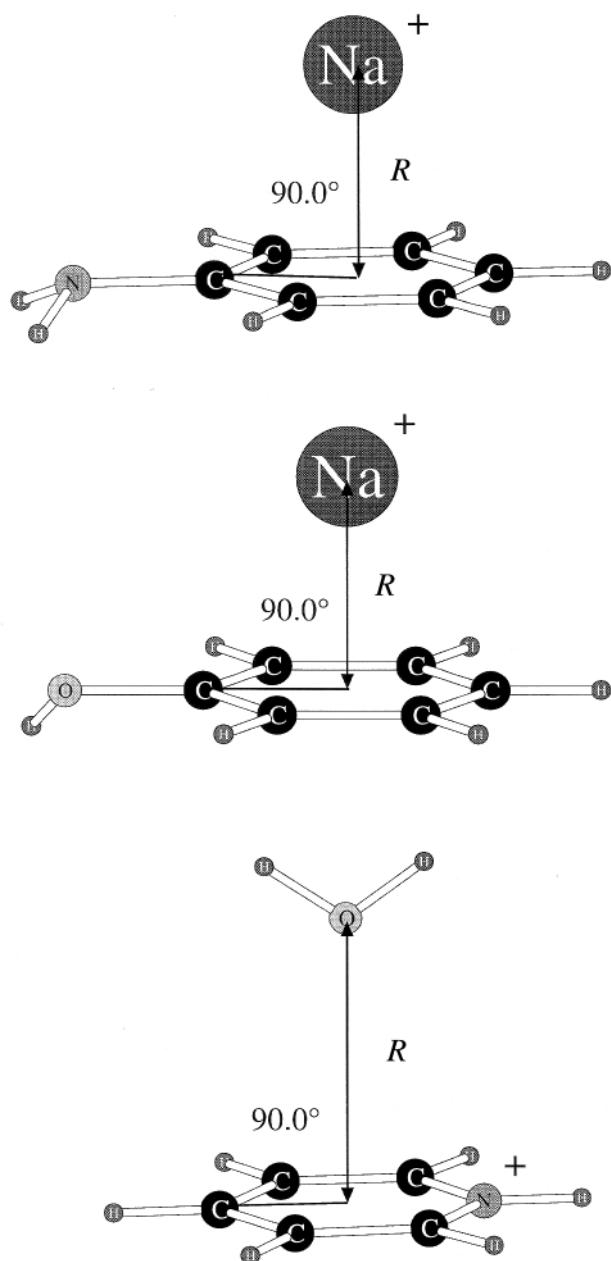
Fig. 1 Na$^+$–aniline, Na$^+$–phenol, and H$_2$O–pyridinium ion complexes used to test the polarizable force field. In all cases, vector **R** originates at the center of the ring and is perpendicular to it. The H$_2$O plane was kept perpendicular to the pyridinium ring and passed through the N. Heavy atoms of the rings were kept coplanar.

found that a γ of 0.86 allows the most accurate reproduction of the *ab initio* results with the force field (Table 4). In fact, the agreement between the empirical and MP2/6-31G*//6-31G* results is notable for a model with only one adjustable parameter, γ.

Computational protocol

All the host–guest complexes were optimized in the gas-phase and the resulting structures were used as starting geometries for the simulations of the solution. The gas-phase optimizations and Monte Carlo simulations were carried out on Silicon Graphics workstations using the BOSS program, version 3.6 modified to account for the polarization interactions and to include the V_4 term in the torsional energy expression.[23] In order to determine relative free energies of association in solution, free energy perturbation (FEP) calculations were run in *ca.* 10 windows to convert the -NH$_2$ to -OH groups in the guests. The following thermodynamic cycle was used and $\Delta\Delta G$

Table 4 Results for representative gas-phase complexes (energies in kcal mol^{-1}, distances in Å)

Property	Na$^+$–C$_6$H$_6$	Na$^+$–Aniline	Na$^+$–Phenol	H$_2$O–pyr$^+$
ΔE(*ab initio*)^a	−29.3	−34.6	−29.3	−8.44
R(*ab initio*)^a	2.45	2.44	2.46	3.19
ΔE(MM)^b	−27.3	−36.0	−30.3	−8.92
E(pol)^b	−14.2	−18.0	−19.2	−1.44
R(MM)^b	2.44	2.42	2.51	3.06

^{a} MP2/6-31G*//6-31G*. ^{b} Molecular mechanics force field including electrostatic polarization.

was obtained *via* eqn. (17).[1] ΔG_3 and ΔG_4 were computed through statistical perturbation theory (SPT).[24,25]

$$\Delta\Delta G = \Delta G_2 - \Delta G_1 = \Delta G_4 - \Delta G_3 \qquad (17)$$

Each MC run consisted of *ca.* 5×10^5 configurations without solute moves to equilibrate the solvent structure, followed by at least 10^6 configurations of equilibration with the full intra- and intermolecular motions allowed for both the solvent and the solutes. At least 5×10^6 additional configurations were used for averaging the results. The starting and ending structures, which correspond to the physically meaningful systems (complexes **1**–**2**, **1**–**3**, **1**–**4**, and **1**–**5**), were run for 6–10×10^6 configurations to test the stability of the complexes and to obtain better equilibrated starting geometries for the subsequent FEP runs. Each liquid simulation involved 500 OPLS CH$_3$CN molecules.[26] The PF$_6^-$ counterions were initially placed symmetrically near the host, when they were included. All solvent–solvent and solvent–solute interactions were truncated spherically at 12 Å separation with quadratic smoothing over the last 0.5 Å. The cutoffs were based on C^1 of acetonitrile and a well-distributed set of non-hydrogen atoms for the host and guests. A standard correction was made to the energy for not including Lennard-Jones interactions beyond the cutoff radius.[27] The ranges for the variations of the internal degrees of freedom and for the rotational and translational movements of the host, guest, counterions, and the solvents molecules were adjusted to produce a *ca.* 40% acceptance rate for new configuration. In all cases, the isothermal–isobaric ensemble (NPT) was employed at 25 °C and 1 atm (0.1013 MPa).
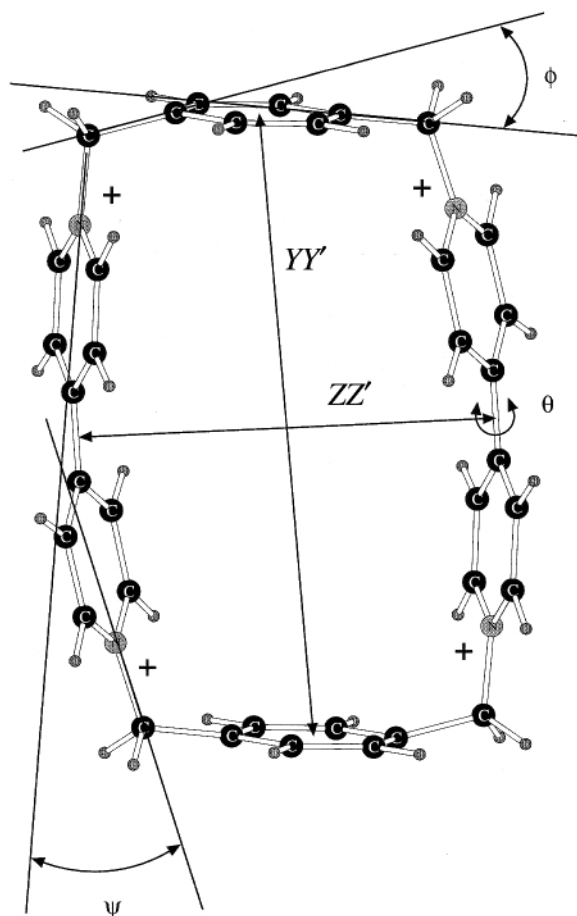
Results and discussion

Gas-phase structures and energies

First, optimizations of the cyclobis(paraquat-*p*-phenylene) host were carried out with and without the PF$_6^-$ counterions and with and without the non-additive polarization term. The energy minima corresponding to centrally symmetric geometries of the host were sought. A typical structure is presented in Fig. 2, which also designates five geometrical parameters whose optimized values along with the experimentally observed[8] and 6-31G* optimized ones[13] are given in Table 5. It can be seen that the force field reproduces the key geometrical parameters well. The only result which is not in close agreement with the experimental data is the angle θ describing the twisting

Table 5 Results of gas-phase optimizations for host **1**[a] (distances in Å, angles in degrees)

System						
Polarization	PF_6^-	ZZ'	YY'	θ	φ	ψ
n	n	7.0	10.5	20	20	22
n	y	6.9	10.4	19	20	22
y	n	7.1	10.4	33	20	24
y	y	7.2	10.4	34	20	24
6-31G*[b]		7.7	10.0	29	—	—
Experiment[c]		6.8	10.3	19	14	23

[a] For the meaning of the geometric parameters see Fig. 2. [b] Ref. 13. [c] Ref. 6.

Table 6 Energetic results of gas-phase optimizations for complexes **1–2** and **1–3** in kcal mol^{-1}

System	Polarization	ΔE_{total}[a]	ΔE_{def}[b]	ΔE_{XX}[c]	ΔE_{pol}[d]
1–2 sym.	n	−30.83	3.61	−34.44	—
1–2 offset	n	−23.29	6.92	−30.21	—
1–3 sym.	n	−24.84	1.76	−26.59	—
1–3 offset	n	−15.70	7.00	−22.70	—
1–2 sym.	y	−34.82	3.05	−34.69	−3.17
1–3 sym.	y	−26.57	2.52	−24.34	−4.75

[a] Energy of complex formation computed as difference between the total energy of the complex and total energies of the separate components. [b] Energy of deformation (bond stretching, angle bending, torsional energy and the intramolecular non-bonded interactions). [c] Additive solute–solute interaction energy. [d] Non-additive electrostatic polarization energy.

Table 7 Energetic results in kcal mol^{-1} of gas-phase optimizations for complexes **1–4** and **1–5**[a]

System	Polarization	ΔE_{total}	ΔE_{def}	ΔE_{XX}	ΔE_{pol}
1–4	n	−24.48	3.16	−27.64	—
1–4	y	−25.70	2.62	−27.01	−1.30
1–5	n	−24.16	2.78	−26.94	—
1–5	y	−22.98	2.70	−26.64	0.96

[a] Same definitions as in Table 6.

Fig. 2 Optimized gas-phase host structure (no polarization, no counterions). Resultant values of the geometric parameters YY', ZZ', θ, φ, and ψ for this and other gas-phase optimizations of the isolated host are given in Table 5.

of the pyridinium rings of the host with respect to each other. The 6-31G* result for this angle is also high, so crystal packing may be contributing to the discrepancies.

Structural and energetic results from optimizations of the complexes of cyclobis(paraquat-*p*-phenylene) with benzidine, biphenol, diaminobenzene, and hydroquinone are shown in Figs. 3–5 and Tables 6 and 7. Geometries of the gas-phase complexes did not depend much on including polarization, thus only one representative structure for each complex type is illustrated. The optimized complexes all reflect substantial inclusion of the guests in the central cavity of the host. Complexes of cyclobis(paraquat-*p*-phenylene) with benzidine (**1–2**) and with biphenol (**1–3**) were optimized in the gas-phase with and without polarization. They were optimized starting in a symmetric form with the center of symmetry inside the host and in a non-symmetric alternative with the guests offset from the centrally-symmetric position (Figs. 3 and 4, respectively). All

the structures were found to be true energy minima, so that no constraints were needed.

The geometry of the **1–2** complex (Fig. 3a) is characteristic of all the symmetric **1–2** complexes in the gas-phase. The energetics without and with polarization are similar for the non-bonded (Coulomb plus Lennard-Jones) host–guest interactions (−34.44 and −34.69 kcal mol^{-1} in Table 6). The deformation contributions to the association energies also have similar values of 3.61 and 3.05 kcal mol^{-1}, so that the difference in the total energies of association, −30.83 *vs.* −34.82 kcal mol^{-1}, comes mostly from the polarization energy of −3.17 kcal mol^{-1} in the latter case.

Turning to the non-symmetric **1–2** complex (Fig. 4a), the center of one of the aromatic rings of the guest is located close to the center of the host. The net association energy for the offset complex with benzidine (−23.29 kcal mol^{-1}) is notably less favorable than the energy for the corresponding symmetric complex (−30.83 kcal mol^{-1}) given in Table 6. This difference comes about evenly from the deformational and intersolute non-bonded interactions.

The symmetric complexes of **1** with biphenol (**1–3**) are geometrically similar to the **1–2** complexes (Fig. 3b). While the non-polarizable symmetric **1–3** complex was found to have a total additive host–guest interaction of −26.59 kcal mol^{-1}, its polarizable counterpart yielded a corresponding value of −24.34 kcal mol^{-1} (Table 6). This decrease in the pairwise binding energy is partly compensated by the polarization effects, which are greater for the **1–3** complexes (−4.75 kcal mol^{-1}) than with the benzidine guest (−3.17 kcal mol^{-1}). The polarizable symmetric **1–3** complex also pays a higher price in deformation energy (2.52 kcal mol^{-1}) for the association than the non-polarizable one (1.76 kcal mol^{-1}). The higher polarization effect for the biphenol complexes *vs.* the benzidine ones can probably be explained by the stronger local electrostatic field produced by the hydroxy groups of the guest. Thus, the greater polarization effect is due to stronger polarization of the host rather than of the guest.

The geometry of the offset **1–3** complex is also similar to that of the **1–2** analog (Fig. 4b). The total energy of association (−15.70 kcal mol^{-1}, Table 6) is 9.14 kcal mol^{-1} higher than for the corresponding symmetric complex (*vs.* 7.54 kcal mol^{-1} in
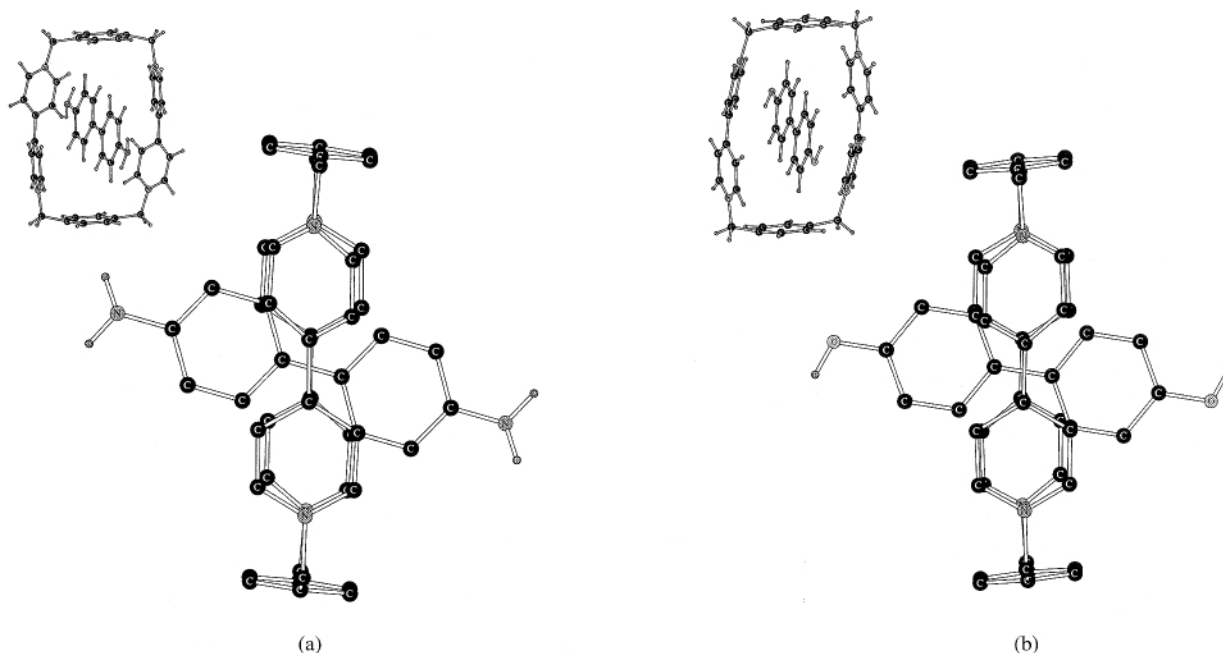
Fig. 3 Typical structures of gas-phase optimized symmetric **1**–**2** (a) and **1**–**3** (b) complexes.
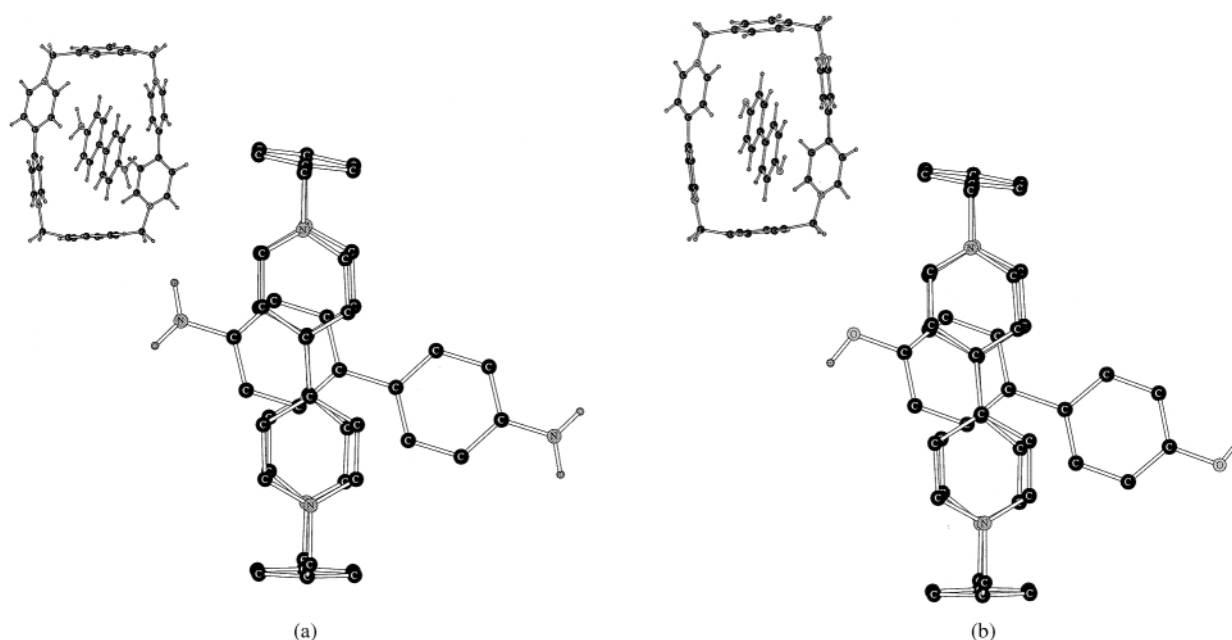

Fig. 4 Typical structures of gas-phase optimized offset **1**–**2** (a) and **1**–**3** (b) complexes.

the benzidine case). The deformation energy of 7.00 kcal mol^{-1} is also significantly higher than the deformation energy of the symmetric system. The total host–guest interaction energy of -22.70 kcal mol^{-1} is 3.89 kcal mol^{-1} higher than for the symmetric form (4.23 kcal mol^{-1} for the benzidine complex). The general trend from the optimizations that the **1**–benzidine complexes are more stable is in-line with experimental data showing a higher association constant for the **1**–**2** complex than for the **1**–**3** one (1044 M^{-1} *vs.* 140 M^{-1}),[10] though solvation remains to be considered in the calculations.

Representative optimized structures for the cyclobis-(paraquat-*p*-phenylene) complexes with the disubstituted benzenes, diaminobenzene **4** and hydroquinone **5**, are shown in Fig. 5 with their energetic data in Table 7. The NH$_2$ and OH groups are now located close enough on the guests so that they can simultaneously interact with the pyridinium nitrogens of the host. Once again, including polarization has no significant effect on the structure of the **1**–diaminobenzene complex (Fig.

5a). The energetics (Table 7) also do not undergo substantial changes. The total host–guest non-bonded interaction energy changes from -27.64 to -27.01 kcal mol^{-1} as the polarization is added with the Coulombic and Lennard-Jones components going from -12.95 to -12.86 and from -14.68 to -14.15 kcal mol^{-1}, respectively. The deformation energy decreases slightly from 3.16 to 2.62 kcal mol^{-1}, so that the total lowering of the association energy from -24.48 to -25.70 kcal mol^{-1} is largely due to the emerging polarization attraction of -1.30 kcal mol^{-1}.

Polarization is also the major factor in changing the **1**–**5** complexation energy from -24.16 to -22.98 kcal mol^{-1}. While the deformation energies for the complexes with and without polarization are very close (2.70 and 2.78 kcal mol^{-1}, respectively) and so are the additive host–guest interactions (-26.64 and -26.94 kcal mol^{-1}), the polarization energy of 0.96 kcal mol^{-1} is responsible for the complex with polarization becoming slightly less stable. This result presages an increase in the

Table 8 Results of the FEP calculations for the **1**–**2** to **1**–**3** and **1**–**4** to **1**–**5** mutations in CH_3CN (energies in kcal mol^{-1})^a

Perturbation	Polarization	PF_6^-	ΔG_3 (unbound)	ΔG_4 (bound)	Calc. $\Delta\Delta G$	Exptl. $\Delta\Delta G^b$
1–**2**→**1**–**3**	n	n	-0.98 ± 0.14	0.51 ± 0.19	1.49 ± 0.23	1.19
1–**2**→**1**–**3**	y	n	-0.98 ± 0.14	-0.59 ± 0.22	0.39 ± 0.26	1.19
1–**2**→**1**–**3**	n	y	-0.98 ± 0.14	0.98 ± 0.17	1.96 ± 0.21	1.19
1–**2**→**1**–**3**	y	y	-0.98 ± 0.14	-0.20 ± 0.15	0.78 ± 0.20	1.19
1–**4**→**1**–**5**	n	n	-1.14 ± 0.14	0.20 ± 0.12	1.34 ± 0.18	1.09
1–**4**→**1**–**5**	y	n	-1.14 ± 0.14	0.28 ± 0.15	1.42 ± 0.20	1.09

^{a} Statistical uncertainties computed with the batch means procedure. ^{b} Refs. 10, 11.

(a)   (b)
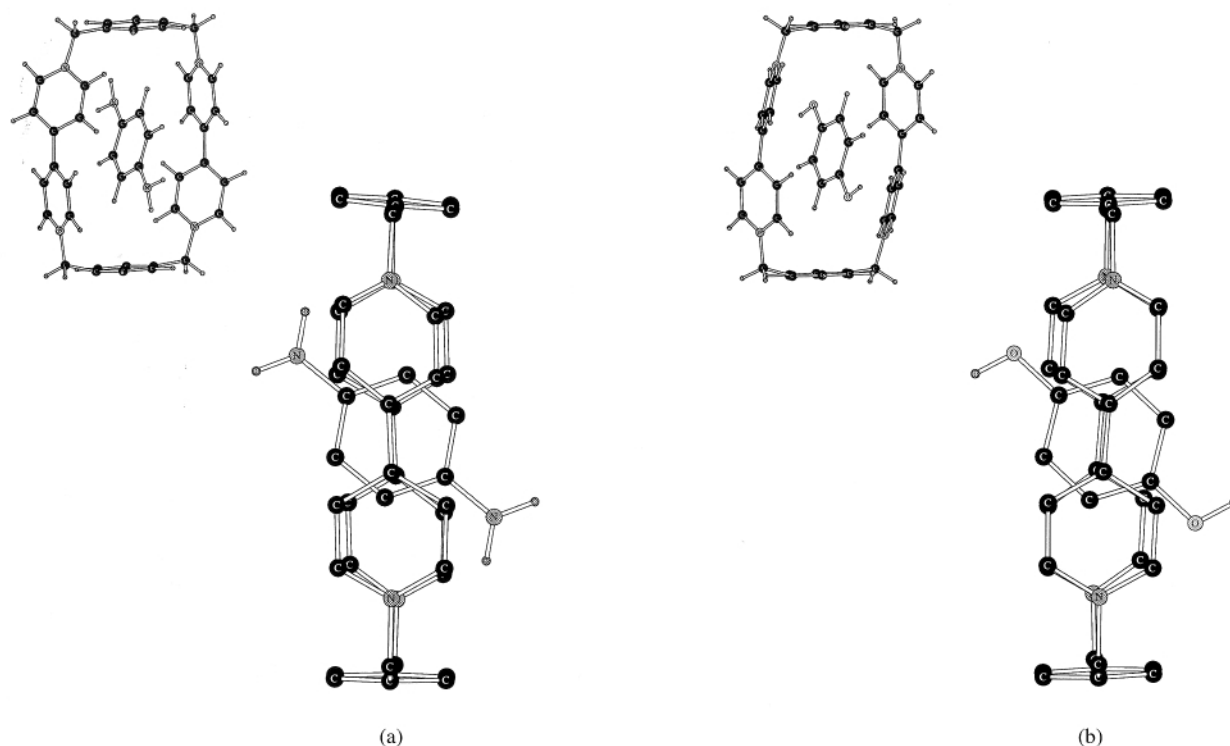
Fig. 5 Typical structures of gas-phase optimized symmetric **1**–**4** (a) and **1**–**5** (b) complexes.

free energy of association difference for the **1**–**4** and **1**–**5** complexes in acetonitrile after including polarization. It may also be noted that the lessened influence of polarization on the complexation energetics for the disubstituted benzenes than the biphenyls is consistent with prior quantum mechanical results.[13]

The optimized symmetric complexes were used as starting points for the calculations in solution. Any biases from this choice should be removed during the initial equilibration part of the Monte Carlo computations.

Liquid-phase Monte Carlo simulations

Perturbations in acetonitrile solution have been carried out from the cyclobis(paraquat-*p*-phenylene) complex with the benzidine guest to the complex with the biphenol guest using the force fields including and excluding the polarization, and with and without the PF_6^- counterions. Perturbations from complexes of **1** with diaminobenzene to its hydroquinone analogue (**1**–**4** to **1**–**5**) were also performed with and without the polarization but with no PF_6^- ions. Monte Carlo simulations of the **1**–**2**, **1**–**3**, **1**–**4**, and **1**–**5** complexes in CH_3CN had been run before starting the FEP calculations. Representative structures from the MC simulations are given in Figs. 6 and 7. Free energy differences obtained for the mutations are given in Table 8.

Liquid-phase NMR data suggest that the cyclobis(paraquat-*p*-phenylene) complex with benzidine **2** is either quite close to the symmetric form similar to the geometries shown on Fig. 3a,

or that the average structure is close to this form, while the guest may be actually moving back and forth inside the host.[10] In the calculations, the guest stayed inside the host's cavity for several million MC configurations but finally came to a more protruding position in all cases. Fig. 8 shows snapshots from the simulations of the **1**–**2** complex without polarization after different numbers of configurations. The guest stayed close to the symmetric position for about 6 million configurations, but then it finally shifted outward. An entropic term is expected to favor the offset structures in solution since they represent a larger fraction of the available configuration space than the symmetrical structures. The offset structures may also be expected to be favored by better enthalpic solvation of the more exposed host and guest.

The structural behavior of the **1**–**2** complex in acetonitrile did not depend on whether the counterions were included or not, the guest drifted to the shifted position in all cases. Inclusion of polarization yielded the same outcome too. These results are, in fact, consistent with the experimentally determined crystal structure of the **1**–**2** complex.[28] Fig. 9 shows the X-ray structure, which is notably similar to the endpoints from the liquid-phase simulations (Figs. 6 and 8).

The observation that the host–guest complex prefers at least one polar group of the guest to be close to the host cavity is supported by the structural results of the simulations of the **1**–**4** and **1**–**5** complexes. In these cases the polar NH_2 or OH groups of the guests can have favorable electrostatic interactions with the positively charged host simultaneously. Thus,
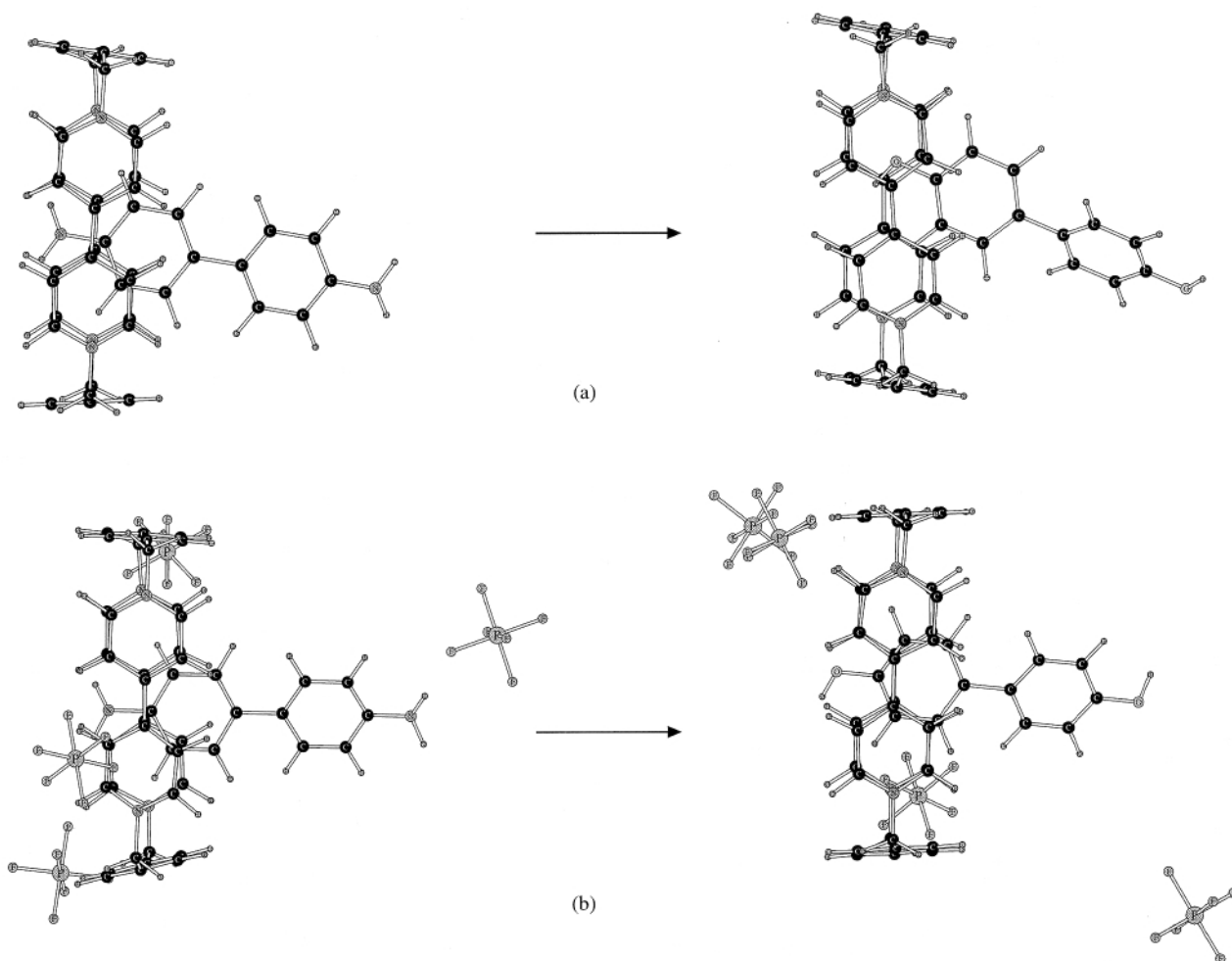
Fig. 6 Representative structures of the **1–2** and **1–3** complexes in CH$_3$CN without (a) and with (b) the PF$_6{}^-$ counterions.

these complexes are much closer to being centrally symmetric than the former ones (Fig. 7). In fact, the guests **4** and **5** drifted little from their positions in the gas-phase optimized structures (Fig. 5).

These structural results clearly show the advantage of the Monte Carlo simulations over simple energy minimizations. The energy minimum for the **1–2** complex has the benzidine guest positioned symmetrically inside the host cavity. One might assume this shape of the complex to also be the predominant one in the liquid phase and thus use it in continuum solvation calculations or for optimizing the complex in the presence of just a few solvent molecules.[13] However, the Monte Carlo simulations of the **1–2** complexes in solution indicate that this geometry is metastable, the guest eventually shifts outward, as in the crystal structure.

The relative ΔG's of association for the **1–2** and **1–3**, and **1–4** and **1–5** complexes calculated with different models are compared with the available experimental data in Table 8.[10,11] While inclusion of the polarization interactions does not alter significantly the structural properties, the energetic results are somewhat affected. $\Delta\Delta G$ of association of **1** with benzidine and biphenol including the PF$_6{}^-$ counterions is overestimated by 0.8 kcal mol^{-1} without the polarization (1.96 vs. 1.19 kcal mol^{-1}), while including the polarization yields a result closer to the experimental one (0.78 kcal mol^{-1}). Taking into account the counterions also raises $\Delta\Delta G$ in both cases (1.49 vs. 1.96 and 0.39 vs. 0.78 kcal mol^{-1} without and with the polarization, respectively). Overall, the computed $\Delta\Delta G$ values for the **1–2** and **1–3** complexes are all qualitatively reasonable; the small quantitative error for the result with the polarization and counterions is gratifying.

Including polarization for the diaminobenzene and hydro-

quinone guests increases the magnitude of the $\Delta\Delta G$ from 1.34 to 1.42 kcal mol^{-1}, though the difference is within the statistical uncertainties. Both results are in excellent accord with the experimental difference of 1.09 kcal mol^{-1} (Table 8).

A final issue to expand on about the force field is the source of the electrostatic charges for the diaminobenzene and hydroquinone molecules. While the utilized charges for the NH$_2$ and OH groups reproduce well observed properties of liquid aniline and phenol,[29] disubstituted benzenes were studied in this work and thus the aniline- and phenol-based OPLS electrostatic charges may be not entirely adequate. To test the sensitivity of host–guest interactions in the **1–4** and **1–5** complexes an additional gas-phase study was undertaken. The diaminobenzene and hydroquinone molecules were optimized with the GAUSSIAN92 program using the 6-31G* basis set. Values of the CHELPG/OPLS charges (in electrons) are shown below.
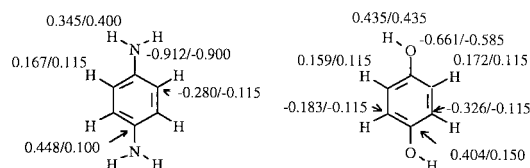
Although the CHELPG and OPLS charges for the NH$_2$ and OH groups themselves are quite similar, the atoms of the phenyl rings have different charges, especially the *ipso* carbon atoms. The OPLS charge for these atoms in diaminobenzene is only +0.100 electron, while the CHELPG charge is +0.448 e. It should also be pointed out that there is a significant asymmetry in the hydroquinone charge distribution. All the non-*ipso*
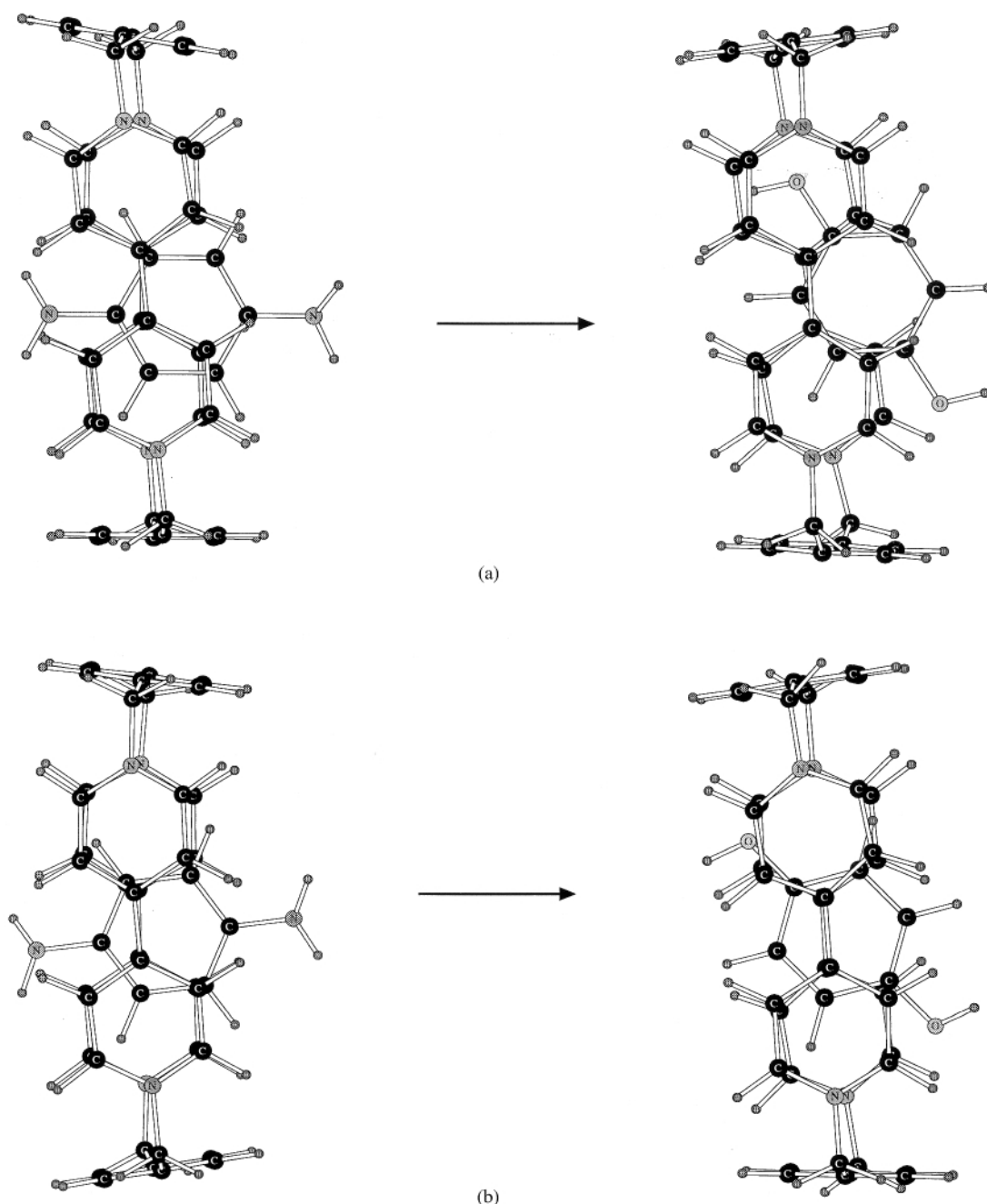
Fig. 7 Representative structures of the **1**–**4** and **1**–**5** complexes in CH₃CN without (a) and with (b) the electrostatic polarization.

phenyl carbons are equivalent in the OPLS approach, yet their CHELPG charges are different (-0.326 e for the carbons *cis* to the hydroxy hydrogens and -0.183 e for the other two). This difference may be unimportant in modeling bulk properties, but it may affect local host–guest interactions. It may also just be an artifact of the EPS-fitting procedure.

In any event, complexes **1**–**4** and **1**–**5** were optimized with and without polarization using both the OPLS and 6-31G* CHELPG charges for the guests. The structures of the complexes are the same as in Fig. 5. The association energy for **1**–**4** changes from -24.48 to -22.33 kcal mol⁻¹, when the OPLS charges are replaced by the CHELPG ones without polarization, and from -25.70 to -23.21 with polarization included. The corresponding changes for the **1**–**5** complexes are from -24.16 to -17.72 kcal mol⁻¹ and from -22.98 to -18.85 kcal mol⁻¹, respectively. Though the differences would be damped in solution, the significantly larger intrinsic difference between the **1**–**4** and **1**–**5** complexes with the CHELPG charges would likely yield larger $\Delta\Delta G$ values and poorer accord with the experimental data in Table 8.

Conclusion

Results of calculations on complexes of cyclobis(paraquat-*p*-phenylene) with benzidine, biphenol, 1,4-diaminobenzene, and hydroquinone in the gas-phase and in CH₃CN solution with molecular mechanics and Monte Carlo simulations have been reported. The complexes were chosen for their importance as basic structural elements in a wide variety of rotaxanes and catenanes and for their prospective use in nanoscale molecular devices. Net association energies of the donor–acceptor pairs in the gas phase and their relative free energies of association in acetonitrile solution were computed with an all-atom molecular force field including electrostatic polarization as well as with the standard OPLS-AA force field. Both approaches gave similar structural results in agreement with available X-ray data and relative free energies of binding in good accord with experiment. However, inclusion of the polarization in acetonitrile lowered the magnitude of $\Delta\Delta G$ for the benzidine–biphenol pair from 1.96 to 0.78 kcal mol⁻¹ with the PF₆⁻ counterions included and improved the accord with the experimental value

4M

6M

10M
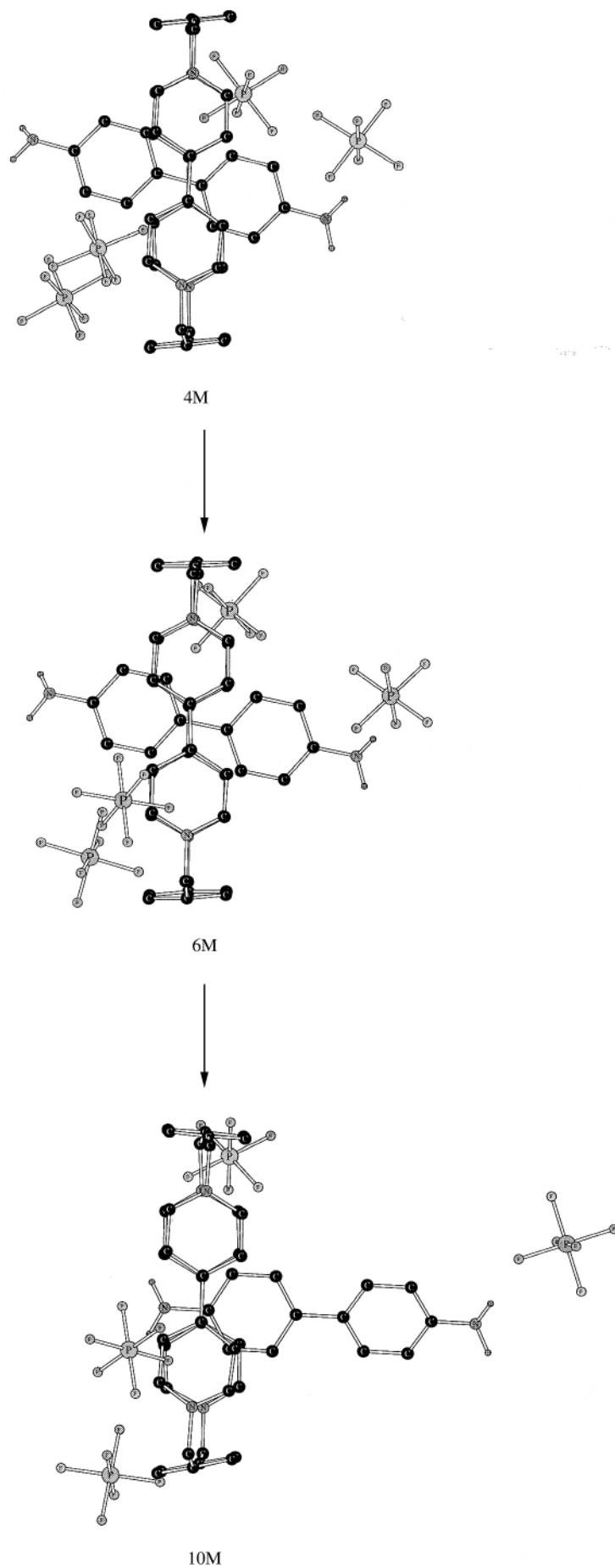
Fig. 8 Snapshots of the complex of **1** with benzidine after the indicated numbers of Monte Carlo configurations in CH₃CN without polarization.
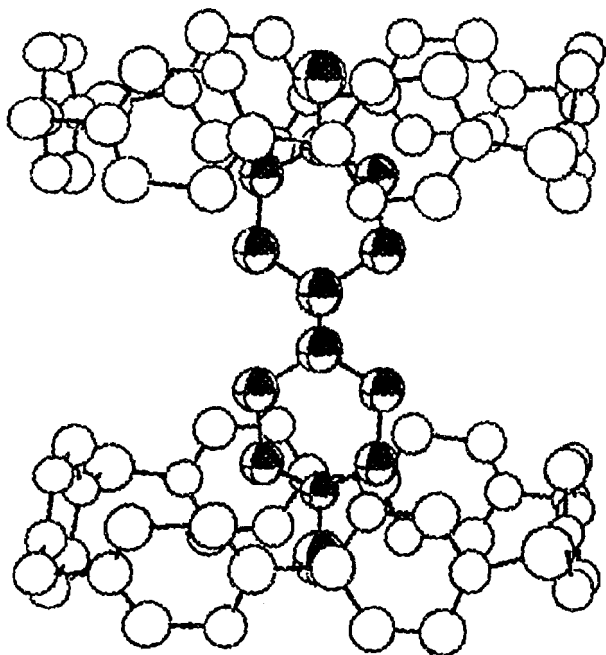
Fig. 9 X-Ray crystal structure of cyclobis(paraquat-*p*-phenylene)[4+] complex with benzidine (ref. 28).

of 1.19 kcal mol^{−1}. At the same time, including the polarizability made the absolute value of the free energy difference slightly greater for the 1,4-diaminobenzene–hydroquinone pair. Overall the force field including non-additive electrostatic polarization appears suitable for further modeling of rotaxanes, catenanes, and related molecular systems. Hopefully, this success will encourage further computational studies of similar complexes and a better understanding of their structural and energetic properties.

Acknowledgements

References

1 (*a*) C. L. Brooks, III, M. Karplus and B. M. Pettitt, *Adv. Chem. Phys.*, 1988, **71**, 1; (*b*) W. L. Jorgensen, *Acc. Chem. Res.*, 1989, **22**, 184; (*c*) P. A. Kollman, *Chem. Rev.*, 1993, **93**, 2395.
2 J. W Caldwell and P. A. Kollman, *J. Am. Chem. Soc.*, 1995, **117**, 4177.
3 D. N. Bernardo, Y. Ding, K. Krogh-Jespersen and R. M. Levy, *J. Phys. Chem.*, 1994, **98**, 4180.
4 (*a*) C. J. F. Böttcher, *Theory of Electric Polarization*, 2nd edn., Elsevier, Amsterdam, 1973; (*b*) B. Roux, *Chem. Phys. Lett.*, 1993, **212**, 231; (*c*) B. Roux and M. Karplus, *J. Comput. Chem.*, 1995, **16**, 690.
5 L. X. Dang, J. E. Rice, J. Caldwell and P. A. Kollman, *J. Am. Chem. Soc.*, 1991, **113**, 2481.
6 P. L. Anelli, P. R. Ashton, R. Ballardini, V. Balzani, M. Delgado, M. T. Gandolfi, T. T. Goodnow, A. E. Kaifer, D. Philp, M. Pietraszkiewicz, L. Prodi, M. V. Reddington, A. M. Z. Slawin, N. Spencer, J. F. Stoddart, C. Vicent and D. S. Williams, *J. Am. Chem. Soc.*, 1992, **114**, 193; M. C. T. Fyfe and J. F. Stoddart, *Acc. Chem. Res.*, 1997, **30**, 393.
7 P. R. Ashton, R. Ballardini, V. Balzani, M. Belohradsky, M. T. Gandolfi, D. Philp, L. Prodi, F. M. Raymo, M. V. Reddington, N. Spencer, J. F. Stoddart, M. Venturi and D. J. Williams, *J. Am. Chem. Soc.*, 1996, **118**, 4931.
8 B. Odell, M. V. Reddington, A. M. Z. Slawin, N. Spencer, J. F. Stoddart and D. J. Williams, *Angew. Chem.*, *Int. Ed. Engl.*, 1988, **27**, 1547.
9 (*a*) P. R. Ashton, E. J. T. Chrystal, P. T. Glink, S. Menzer, C. Schiavo, J. F. Stoddart, P. A. Tasker and D. J. Williams, *Angew. Chem.*, *Int. Ed. Engl.*, 1995, **34**, 1869; (*b*) D. B. Amabilino, P. R. Ashton, M. Belohradsky, F. M. Raymo and J. F. Stoddart, *J. Chem. Soc.*, *Chem. Commun.*, 1995, **7**, 751; (*c*) N. Solladie, J. C. Chambron, C. O. Dietrichbuchecker and J. P. Sauvage, *Angew. Chem.*, *Int. Ed. Engl.*, 1996, **35**, 906; (*d*) V. Balzani, M. Gomez-Lopez and J. F. Stoddart, *Acc. Chem. Res.*, 1998, **31**, 405.
10 E. Cordova, R. A. Bissell, N. Spencer, P. R. Ashton, J. F. Stoddart and A. E. Kaifer, *J. Org. Chem.*, 1993, **58**, 6550.
11 A. C. Benniston, A. Harriman, D. Philip and J. F. Stoddart, *J. Am. Chem. Soc.*, 1993, **115**, 5298.
12 P. R. Ashton, C. G. Claessens, W. Hayes, S. Menzer, J. F. Stoddart, A. J. P. White and D. J. Williams, *Angew. Chem.*, *Int. Ed. Engl.*, 1995, **34**, 1862.
13 R. Castro, M. J. Berardi, E. Cordova, M. O. Deolza, A. E. Kaifer and J. D. Evanseck, *J. Am. Chem. Soc.*, 1996, **118,** 10257; R. Castro, M. J. Berardi, E. Cordova, K. R. Nixon, M. O. Deolza, A. E. Kaifer and J. D. Evanseck, *Abstracts of Papers of the American Chemical Society*, 1996, **212**, 160-Comp.; R. Castro, P. D. Davidov, K. A. Kumar, A. P. Marchand, J. D. Evanseck and A. E. Kaifer, *J. Phys. Org. Chem.*, 1997, **10**, 369.
14 F. M. Raymo, K. N. Houk and J. F. Stoddart, *J. Org. Chem.*, 1998, **63**, 6523.
15 S. J. Weiner, D. A. Case, P. A. Kollman and D. T. Nguyen, *J. Comput. Chem.*, 1986, **7**, 230.
16 W. L. Jorgensen, D. S. Maxwell and J. Tirado-Rives, *J. Am. Chem. Soc.*, 1996, **118**, 11225.
17 E. M. Duffy and W. L. Jorgensen, *J. Am. Chem. Soc.*, 1994, **116**, 6337.
18 W. L. Jorgensen and T. B. Nguyen, *Proc. Natl. Acad. Sci. USA*, 1993, **90**, 1194.
19 (*a*) A. Almenningen, O. Bastiansen, L. Fernholt, B. N. Cyvin, S. J. Cyvin and S. Samdal, *J. Mol. Struct.*, 1985, **128**, 59; (*b*) C. Jaime and J. Font, *J. Mol. Struct.*, 1989, **195**, 103.
20 H. A Carlson, T. B. Nguyen, M. Orozco and W. L. Jorgensen, *J. Comput. Chem.* 1993, **14**, 1240.
21 K. J. Miller. *J. Am. Chem. Soc.*, 1990, **112**, 8533.
22 M. J. Frisch, G. W. Trucks, M. Head-Gordon, P. M. W Gill, M. W. Wong, J. B. Foresman, B. G. Johnson, H. B. Schlegel, M. A. Robb, E. S. Replogle, R. Gomperts, J. L. Andres, K. Raghavachari, J. S. Binkley, C. Gonzalez, R. L. Martin, D. L. Fox, D. J. Defrees, J. Baker, J. J. P. Stewart and J. A. Pople, GAUSSIAN92; Gaussian, Inc., Pittsburgh, PA, 1992.
23 W. L. Jorgensen, *BOSS Version 3.6*, Yale University, New Haven, CT, 1995.
24 R. W. Zwanzig, *J. Chem. Phys.*, 1954, **22**, 1420.
25 W. L. Jorgensen, *Chemtracts: Org. Chem.*, 1991, **4**, 91 and references therein.
26 W. L. Jorgensen and C. Ravimohan, *J. Chem. Phys.*, 1985, **83**, 3050.
27 W. L. Jorgensen, J. D. Madura and C. J. Swenson, *J. Am. Chem. Soc.*, 1984, **106**, 6638.
28 A. E. Kaifer, personal communication.
29 W. L. Jorgensen, E. R. Laird, T. B. Nguyen and J. Tirado-Rives, *J. Comput. Chem.*, 1993, **14**, 206.

Paper 9/05160K